International Journal of Engineering & Technology, 4 (1) (2015) 149-160
www.sciencepubco.com/index.php/IJET

doi: 10.14419/ijet.v4i1.4033
Research Paper

Experimental analysis on metallic foams-a response surface methodology approach

Osama I. Abd

Renewable Energy Research Center/University of Anbar, Iraq
E-mail: osama_eng21@yahoo.com

Abstract

This study aimed to fabricate metallic porous materials using powder metallurgy (PM) space-holder technique. In the PM route, Al powder was mixed with different ratios (7%, 10%, and 20%) and sizes (500 and 1000 μm) of sodium chloride granules as space-holder agent. The mixture was then compacted at different compacting pressures (150, 200, and 250 MPa) and then heated to 280 °C for sintering. Subsequently, sodium chloride granules were removed by dissolving in water to obtain the porous structure. Tests were performed on all porous Al specimens, and characteristics such as density and porosity were measured. A statistical approach was used to optimize processing parameters. ANOVA statistical tool was used to obtain the final evaluation of the most significant features, namely, relative density and porosity fraction.

Keywords: *Al Foams; ANOVA; Powder Metallurgy; Space-Holder Technique; Statistical Approach.*

1. Introduction

Porous metals, cellular materials, and foams are materials with interconnected pores. Porous metals denote to metals with a large porosity fraction, whereas the term foam applies to porous metals manufactured through the foaming process [1]. Porous metals have been of increasing interest during recent years because of their unique properties for instance air and water permeability, acoustic properties, good electrical insulating properties, low thermal conductivity, impact energy absorption capacity, high stiffness, and extremely low specific weight [1].

Aluminum foams have been identified as a new material class of considerable interest because of their unique combination of properties, which are presented by their cellular structure and metallic behaviour. Notably, the automotive industry sees a great potential in the use of aluminum foams in light-weight structures for crash energy absorption and noise control. Applications are also to predicted in other areas such as in aerospace, ship, railway, biomedical, and building industry, as well as in filters, silencers, heat exchangers, flame arresters, and for water purification [2], [3].

Numerous fabrication methods can be classified according to the status of the starting metal: liquid, powdered, or ionized. Despite the methods available for the production of porous metals, few are capable of creating open-cell foams [3]. Liquid metallurgy route method involves foaming of molten metal either via using reactant and foaming agent or via inert gas injection in the molten metal. The reactant and the foaming agent are mixed after pretreatment with the melt through mechanical stirrer and are allowed to separate the foaming agent to release gases, thus forming metallic foam. The powder metallurgy (PM) route involves the metal and the foaming agent, which are mixed and compacted. Then, the compacted mass is heated to just above the solidus temperature under pressure. The powder compact of metal and foaming agent can be subsequently hot-rolled to obtain sheets of porous metallic foam. PM route based on using space-holder agents were successfully used to produce partially open-pore metal foams. A wide range of materials like organic, inorganic, and ceramic particles or even metallic hollow spheres could be used as spacer agents in PM space-holder techniques [3], [4]. PM space-holder technique can control the pore characteristics because through of the

following explanations [5]: (1) adjustment of spacer and metal powder mixing ratio results in porous metals with finely controlled porosity, and (2) preparation of sieved spacer particles can narrow the pore size distribution.
In the literature, a number of methods exist for the production of aluminum foam, namely, powder metallurgy, melt–gas injection, melt foaming, investment casting and melt infiltration [6]. Zhao and Sun [7] presented an improvement in the P/M route for an open-cell aluminum foam fabrication, known as sintering dissolution process, which uses space holders in the powder mixture to create a porous structure in the desired compacted mixture. Then, the compacts are sintered, and the spacer is removed during the dissolution stage. Rossella Surace et al. [8] produced Al foams by PM technique, and used DOE and ANOVA analysis technique to identify the most significant control factors that influence the foams: compacting pressure, temperature, and content of SiC. The group obtained optimal parameters of 430 MPa, 750 °C, and 3 wt. %, respectively.
This work aims to fabricate aluminum foams, assess their properties, and optimize the processing parameters of the PM space-holder technique by means of a statistical approach. During the experimental work, multiple specimens have been established. ANOVA statistical tool was used to conduct the final evaluation of the most significant features (relative density and porosity fraction).

2. Experimental procedure

Aluminum powder with an average diameter of 53 μm and NaCl granules (as space-holder agent) with sizes of 500 and 1000 μm were selected as raw materials. Table (1) shows the chemical composition of the Al powder, which was analyzed by Spectro Analytical Instruments Boschstrab 10, D-4190KLEVE. A fixed weight of Al powder is mixed with different ratios (7%, 10%, and 20%) of NaCl granules. The mixture was then compacted at various compacting pressures (150, 200, and 250 MPa). Then, the compacts were heated and sintered at 280 °C for 30 min. Cylindrical porous Al was subsequently obtained by subjecting the sintered compacts to water washing to remove the space-holding NaCl granules.

Table 1: Chemical Composition of Aluminum Powder

Composition	Al	Zn	Cu	Mg	Mn	Fe	Si
wt%	99.134	0.365	0.1648	0.0604	0.002	0.0025	0.0012

3. Microscopic examination

The specimens were first cut and then prepared using standard metallographic procedures. Etching was achieved by immersing each surface of the polished specimens for 30 s in 5% HF + 95% H_2O as etching solution. Finally, the specimens were washed with water and alcohol, and then dried. The specimens were examined using an optical microscope. Image analysis of the specimens was performed using an optical microscope (Carl-Zeiss) equipped with a digital camera.

4. Evaluation of density of the Al foam

Foams obtained are irregularly shaped, and density calculation by conventional method is not feasible. However, density can be calculated by using Archimedes principle. The density of the foam was calculated using the following method.

1) A measuring jar (MJ) was filled with water to a specified amount, e.g., 500 mL. This amount is designated as the initial water level in the MJ.
2) Then, the foam specimen was gradually immersed into the water-containing MJ, and the new water level is recorded.
3) The difference between the initial and final water levels, which gives the actual volume (V in cc) of the foam specimen, was obtained.
4) The foam specimen was weighed, and its mass (m in grams) is recorded.
5) Foam density (ρ_f) is calculated as [ρ_f = m/V (g/cc)].

5. Evaluation of porosity of the Al foam

Porosity also performs a similarly crucial function as density in deciding foam quality. As the density of the foam decreases, porosity also increases. However, instead of the increase in porosity, uniform porosity of the foam is the important parameter. In the metal foam synthesis, the main objective is to develop uniform porosity.
The proportion of porosity was calculated by using S-Image software. The principle of this program is based on the measured areas of pores after fixing the unit of measurement scale on the unit (μm) and inputting the magnification, as shown in Figure (1). After converting the image to a monochrome (black and white), dark pores were calculated as shown in Figure (2). Then, the volume fraction of the pores is calculated by dividing the sum of these areas to the total

area of the image. J-Image program was also used to match the results of the program with the extracted S-Image as shown in Figure (3), which shows the J-Image view. The results of density and porosity are listed in Table (2).

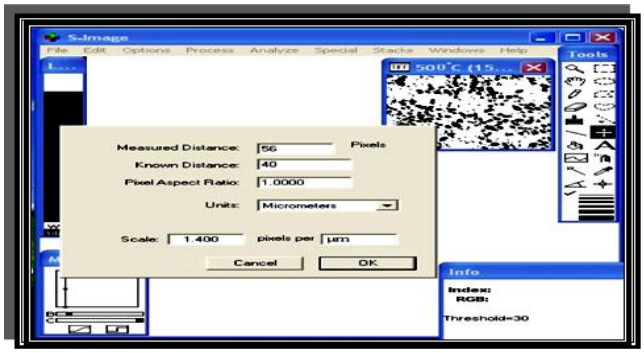

Fig. 1: Image Analysis and Calculation of Pores Areas

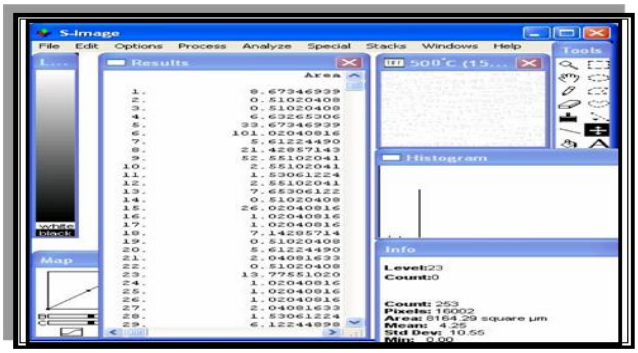

Fig. 2: S-Image View for the Extracted Results

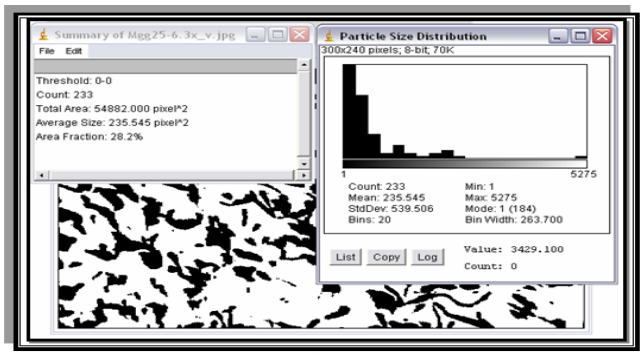

Fig. 3: J-Image View for the Extracted Results

Table 2: Density and %Porosity of Al Foams at Different Conditions

NaCl%	NaCl particle size (µm)	Compacting pressure (MPa)	Density g/cm³	Porosity fraction%
7	500	150	2.61	6
7	1000	150	2.59	6.3
7	500	200	2.65	5
7	1000	200	2.64	5.5
7	500	250	2.66	4.7
7	1000	250	2.65	5.1
10	500	150	2.53	12.4
10	1000	150	2.48	13.3
10	500	200	2.59	11.6
10	1000	200	2.5	12.2
10	500	250	2.59	11.2
10	1000	250	2.51	12.4
20	500	150	2.44	25.2
20	1000	150	2.34	26.6
20	500	200	2.47	22.3
20	1000	200	2.45	24.8
20	500	250	2.47	22.1
20	1000	250	2.46	22.7

6. Design of experiment based on response surface methodology

Response surface methodology (RSM) is conventionally considered in the context of experimental design as a statistical method for modeling and analyzing problems in which different variables affect a response of interest. The first step in RSM includes determining a appropriate approximation for the actual functional relationship between the response variable Y and a set of independent variables as follows: [9].

$$Y = a_0 + \sum_{i=1}^{n} a_i X_1 + \sum_{i=1}^{n} a_{ii} X_1^2 + \sum_{i<j}^{n} a_{ij} X_1 X_2 \quad (1)$$

Where: Y = the predicted response
X_1 and X_2 = independent variables
a_0 = the constant coefficient
a_i and a_j = the linear coefficients
a_{ii} and a_{jj} = the quadratic coefficients
a_{ij} = the interaction coefficient

These coefficients are calculated using an appropriate method, such as the least squares method. When the resulting expected surface is an sufficient approximation of the real response function, the results will be nearly equivalent to the analysis of the actual system. The model parameters can be approached whenever proper experimental designs are used to collect data. In this study, a statistical model is proposed to model the effects of the processing parameters on the performance characteristics of the density and porosity fraction of Al foams. The levels were specified for each parameter as given in the Table (3). Three process parameters at two and three levels resulted in a total of 18 tests for turning operation. After each test, density and volume fraction are calculated as aforementioned. The observations are presented in Table (4) for further analysis and studies.

Table 3: Experimental Parameters and Their Levels

Experimental parameters	Unit	Level 1	Level 2	Level 3
NaCl	%	7	10	20
NaCl particle size	µm	500	-	1000
Compacting pressure	MPa	150	200	250

Table 4: Experimental Parameters and Foaming Responses

Experimental parameters			Response variables	
NaCl	NaCl particle size	Compacting pressure	Density	Porosity fraction
%	µm	MPa	g/cm³	%
A	B	C	D	V
7	500	150	2.61	6
7	1000	150	2.59	6.3
7	500	200	2.65	5
7	1000	200	2.64	5.5
7	500	250	2.66	4.7
7	1000	250	2.65	5.1
10	500	150	2.53	12.4
10	1000	150	2.48	13.3
10	500	200	2.59	11.6
10	1000	200	2.5	12.2
10	500	250	2.59	11.2
10	1000	250	2.51	12.4
20	500	150	2.44	25.2
20	1000	150	2.34	26.6
20	500	200	2.47	22.3
20	1000	200	2.45	24.8
20	500	250	2.47	22.1
20	1000	250	2.46	22.7

7. The results and discussion

7.1. Effect of process parameters

A considerably smaller aluminum powder, with a size of 53 µm, compared with NaCl sizes of 500 and 1000 µm was selected to prevent the fabrication of porous Al with poor mechanical properties. At coarser Al particles, the spacing

NaCl particles consequently prevented Al particles from touching and metallurgically bonding to each other, thus resulting in poor mechanical properties of porous Al [5].

Porous Al specimens were fabricated with different ratios (7%, 10%, and 20%) and sizes (500 and 1000 μm) of sodium chloride granules, at various compacting pressures (150, 200, and 250 MPa), and the compacts were sintered at a fixed sintering temperature of 280 °C and sintering time of 30 min. Figure (4) shows the cross sections of several porous Al specimens fabricated under different conditions. Figure (5) displays the determination results of density (g/m^3) and porosity fraction of porous Al specimens fabricated under various conditions.

The observed readings are plotted in the following graphical illustrations of Figure (5). In general, the density of porous Al decreases with the increase in the wt.% of NaCl spacer granules. Density (ρ_f) decreases as % NaCl increases. In addition, we note that porosity fraction increases as % NaCl increases. At a fixed compacting pressure of 150 MPa and NaCl particle size of 500 μm, the density and porosity fraction are 2.44 g/m^3 and 25.2%, respectively. At a NaCl particle size of 1000 μm, the density and porosity fraction are 2.34 g/m^3 and 26.6%, respectively. Thus, we conclude that with increasing compacting pressure, density increases and porosity fraction decreases with a constant NaCl particle size. At higher compacting pressure, pores coalesce, and thus the porosity fraction decreases. In other words, density increases and porosity fraction decreases as compacting pressure increases with constant NaCl particle size and % NaCl.

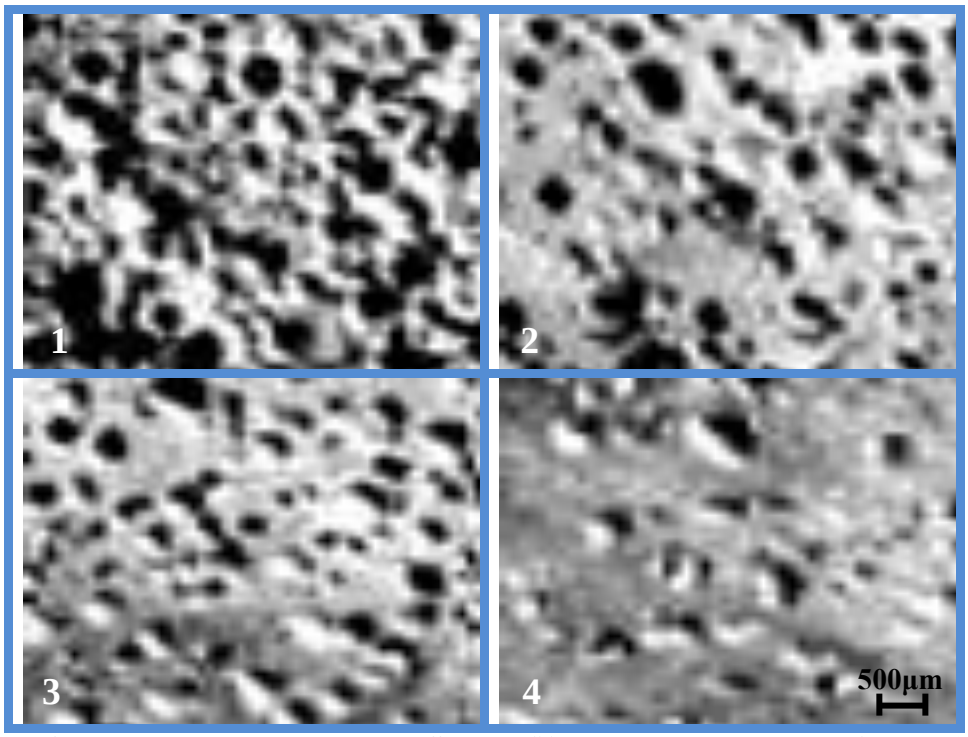

Fig. 4: Cross Sections of Porous Al Specimens Fabricated Under Different Conditions; 1) 20 Wt.% ,1000μm NaCl and 250MPa 2) 10 Wt.%, 1000μm NaCl and 250MPa 3) 20 Wt.%,500μm NaCl and 250MPa 4) 10 Wt.%, 500μm NaCl and 250MPa.

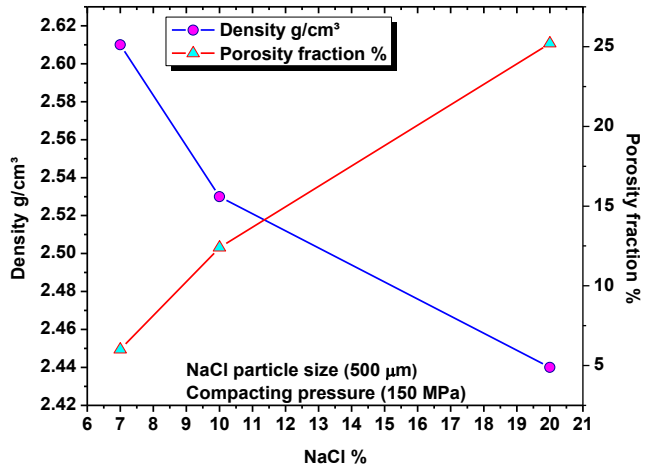

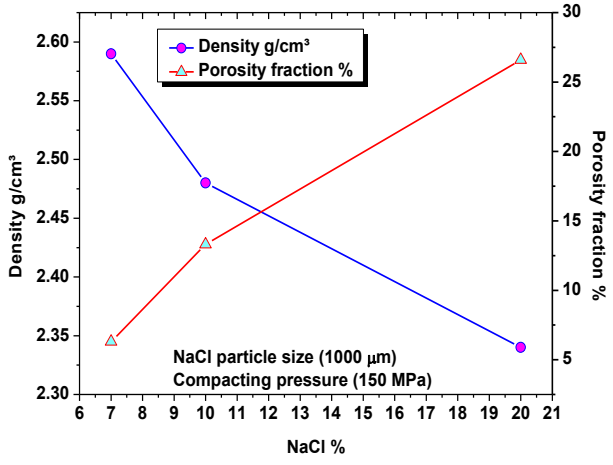

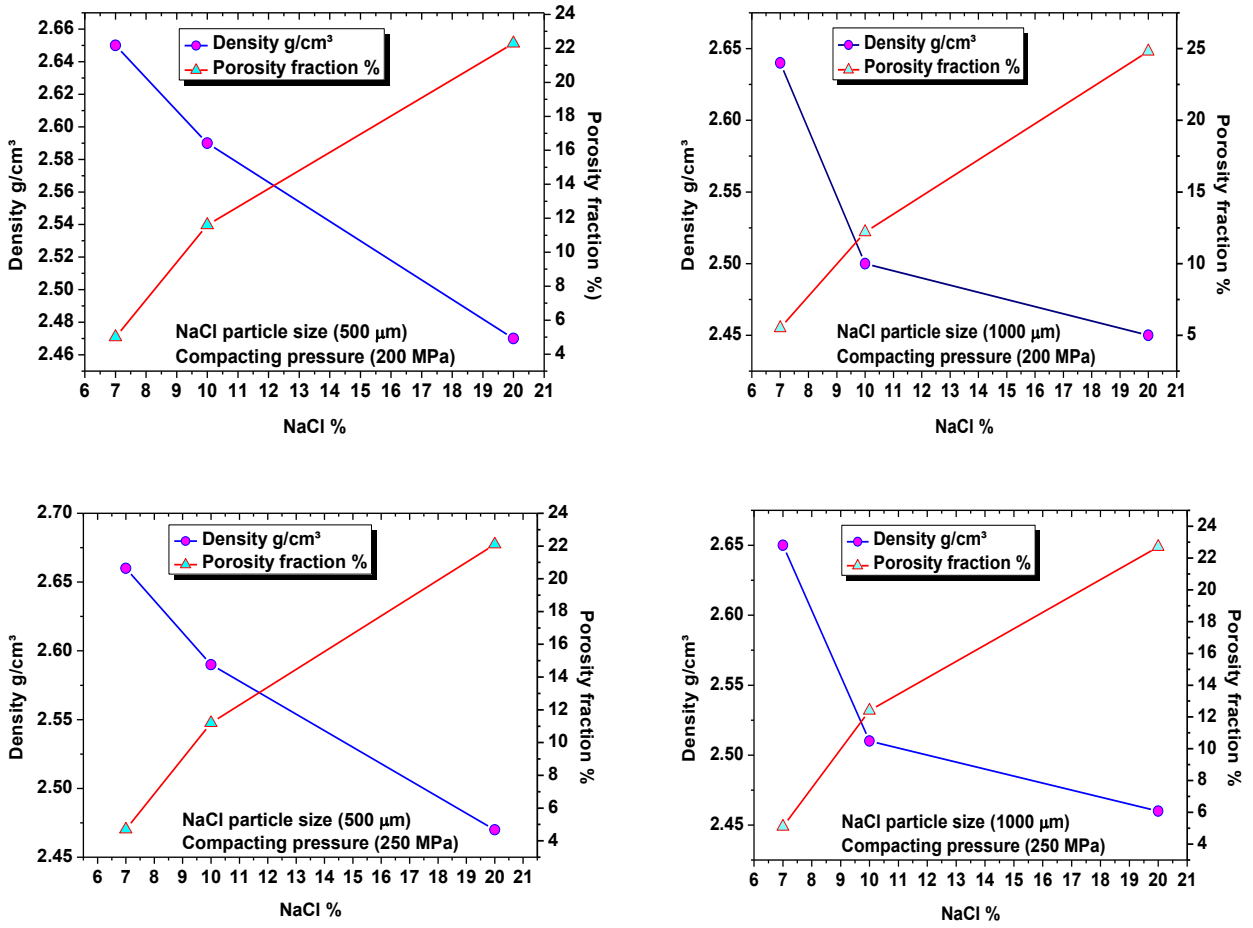

Fig. 5: Shows the Density (g/m^3) and Porosity Fraction (%) of Porous Al Specimens at Different Conditions

7.2. ANOVA and mathematical modeling

Regression analysis of the experimental results was performed using Minitab software ver. 15 (Minitab Inc., State College, PA, USA), and Equation (1) was applied to determine the optimum conditions. In this work, we used two different methods (i.e., graphical and numerical methods) to validate the model. Graphical methods utilize residual analysis between the values of independent variables and predicted values from a regression equation.

7.2.1. Foam density

Table (5) shows the ANOVA table for RSM model for density of fabricated porous Al specimens. The coefficients of regression model are estimated by ANOVA, as shown in Table (6), and analysis was performed using uncoded units. A value of P that is lower than 0.05 indicates that this model is significant. For this model, the value of P (0.000) shows statistically strong significance. The fit of the model was also expressed by coefficient of determination R^2, which was found to be 0.9618, thus indicating good agreement between experimental and predicted values. The mathematical predicted model for density was obtained and is represented by equation (2):

$$Y = 2.69739 - 0.06686A - 0.00016B + 0.00360C + 0.00183A^2 - 0.00001C^2 + 0.00002AC \quad (2)$$

Table 5: ANOVA Table for Response Surface Function of the Density

Source	DF	Seq SS	Adj SS	Adj MS	F	P
Regression	8	0.135660	0.135660	0.016957	28.31	0.000
Linear	3	0.121725	0.018481	0.006160	10.29	0.003
Square	2	0.013059	0.013059	0.006529	10.90	0.004
Interaction	3	0.000876	0.000876	0.000292	0.49	0.699
Residual Error	9	0.005390	0.005390	0.000599		
Total	17	0.141050				
S = 0.0244731	PRESS = 0.0247642					
R-Sq = 96.18%	R-Sq(pred) = 82.44%		R-Sq(adj) = 92.78%			

Table 6: Estimated Regression Coefficients for the Density

Term	Coef.	SE Coef.	T	P
Constant	2.69739	0.231786	11.637	0.000
A: (% NaCl)	–0.06686	0.013311	–5.023	0.001
B: (NaCl particle size, μm)	–0.00016	0.000126	–1.236	0.248
C: (Compacting pressure, MPa)	0.00360	0.002033	1.770	0.110
A*A	0.00183	0.000427	4.292	0.002
C*C	–0.00001	0.000005	–1.839	0.099
A*B	0.00000	0.000004	–0.468	0.651
A*C	0.00002	0.000025	0.750	0.472
B*C	0.00000	0.000001	0.826	0.430

Residuals are defined as the differences between the actual and predicted values for each point in the design. Figure (6) presents randomly distributed residuals and predicted values in a scatter diagram within ± 0.03. In Figure (7), each residual is plotted against an index of observation orders of data, which was used to check for any drift in the process. As previously that shown in Figs. 6 and 7, we were unable to see a pattern of residual distribution. From this result, we may say that each residual is independent. Figure (8) is a graph that checks the normality distribution of the residuals. In this figure, experimental points are near the center cross line, which means the test follows the normal distribution relatively well.

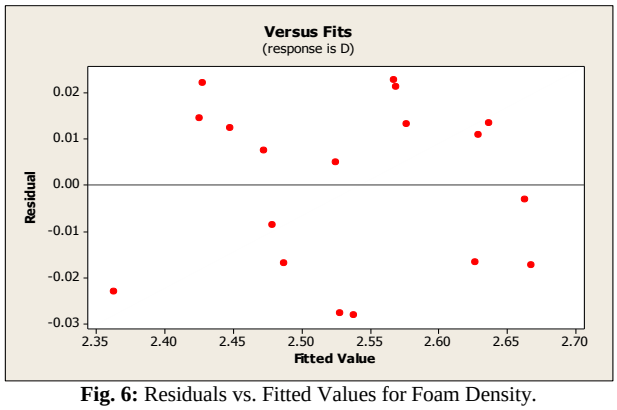

Fig. 6: Residuals vs. Fitted Values for Foam Density.

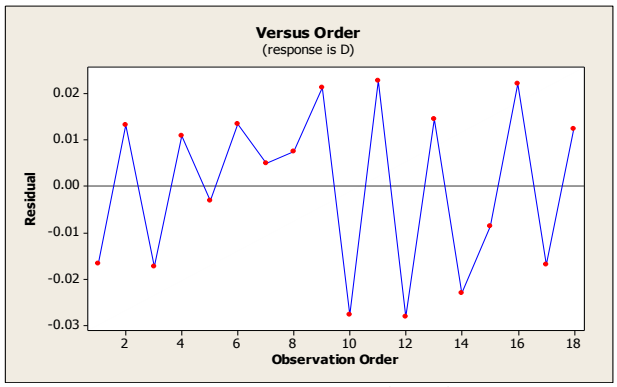

Fig. 7: Residuals vs. Observation Orders of Data for Foam Density.

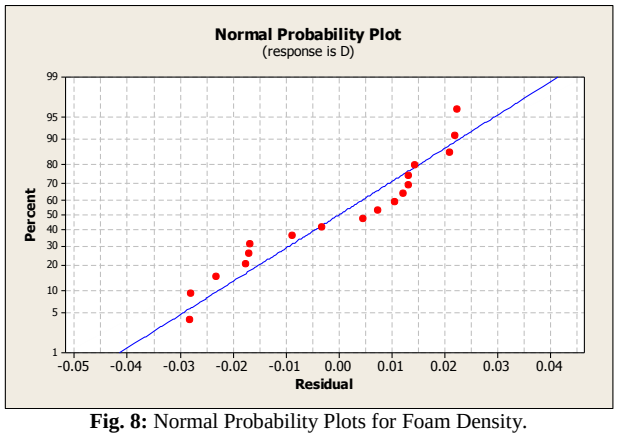

Fig. 8: Normal Probability Plots for Foam Density.

7.2.2. Porosity fraction

Table (7) shows the ANOVA table for RSM model for porosity fraction of the fabricated porous Al specimens. ANOVA estimated the coefficients of regression model, as shown in Table (8), and the analysis was performed using uncoded units. A value of P below 0.05 indicates that this model is significant. For this model, the value of P (0.000) shows statistically strong significance. The fit of the model was also expressed by the coefficient of determination R^2, which was found to be 0.9987, indicating good agreement between experimental and predicted values. The mathematical predicted model for porosity fraction was obtained and is represented by Equation (3):

$$Y = -10.6503 + 3.9183A + 0.0005B - 0.0631C - 0.0826A^2 + 0.0002C^2 + 0.0002AB - 0.0019AC \quad (3)$$

Table 7: ANOVA Table for Response Surface Function of the Porosity Fraction

Source	DF	Seq SS	Adj SS	Adj MS	F	P
Regression	8	1073.91	1073.9075	134.2384	840.77	0.000
Linear	3	1046.52	53.4570	17.8190	111.61	0.000
Square	2	23.13	23.1290	11.5645	72.43	0.000
Interaction	3	4.26	4.2553	1.4184	8.88	0.005
Residual Error	9	1.44	1.4369	0.1597		
Total	17	1075.34				
S = 0.399575	PRESS = 7.61107					
R-Sq = 99.87%	R-Sq(pred) = 99.29%		R-Sq(adj) = 99.75%			

Table 8: Estimated Regression Coefficients for the Porosity Fraction

Term	Coef.	SE Coef.	T	P
Constant	–10.6503	3.78439	–2.814	0.020
A: (% NaCl)	3.9183	0.21733	18.030	0.000
B: (NaCl particle size, μm)	0.0005	0.00206	0.226	0.826
C: (Compacting pressure, MPa)	–0.0631	0.03319	–1.901	0.090
A*A	–0.0826	0.00697	–11.839	0.000
C*C	0.0002	0.00008	2.169	0.058
A*B	0.0002	0.00007	2.314	0.046
A*C	–0.0019	0.00042	–4.606	0.001
B*C	0.0000	0.00001	–0.289	0.779

Figure (9) presents randomly distributed residuals and predicted values in a scatter diagram within ± 0.75. In Figure (10), each residual is plotted against an index of observation orders of data, which was used to check for any drift in the process. As is previously shown in Figs. 9 and 10, we did not see any pattern of residual distribution. From this result, we may say that each residual is independent. Figure (11) is a graph to check the normality distribution of the residuals. In this figure, experimental points are near the center cross line, which means that the test follows a normal distribution relatively well.

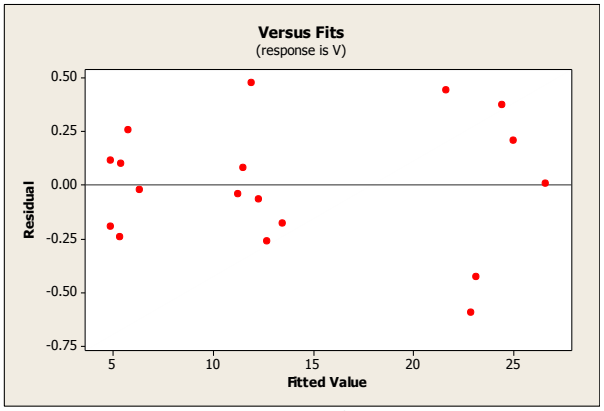

Fig. 9: Residuals vs. Fitted Values for Pore Porosity Fraction.

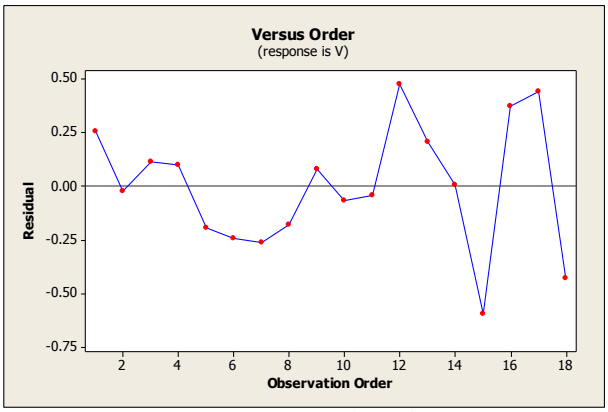

Fig. 10: Residuals vs. Observation Orders of Data for Pore Porosity Fraction.

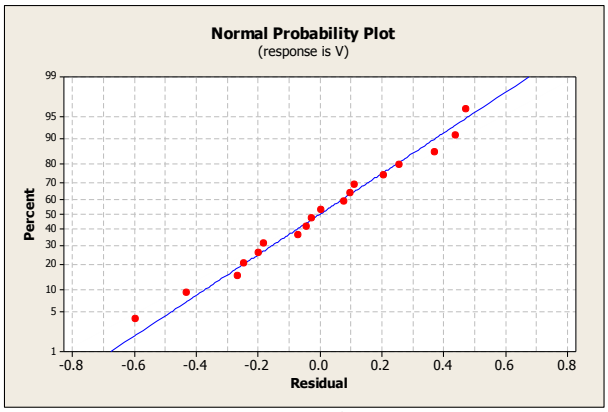

Fig. 11: Normal Probability Plots for Pore Porosity Fraction.

7.3. Process optimization

Identifying an optimal setting involved the following: minimizing foam density and maximizing porosity fraction. The goal values are selected as 2.25 g/cm³ and 25%, respectively. The predicted responses are calculated, as given in Table (9), using global solution factor levels. The predicted responses are the responses expected if global solution factor levels were used.

Table 9: Predicted Responses for Density and Porosity Fraction

NaCl %	NaCl particle size µm	Compacting pressure MPa	Density g/cm³	Porosity fraction %	Desirability
18.0303	1000	150	2.35568		0.742236
20	1000	150		26.5946	1.000000

In Figure (12), a two-contour line graph shows the effects on foam density based on % NaCl, NaCl particle size, and compacting pressure. Figure (13) displays the optimum value at the top of the graph at 18.0303%, 1000 µm, and 150 MPa, with a resulting minimum foam density of 2.35568 g/cm³.

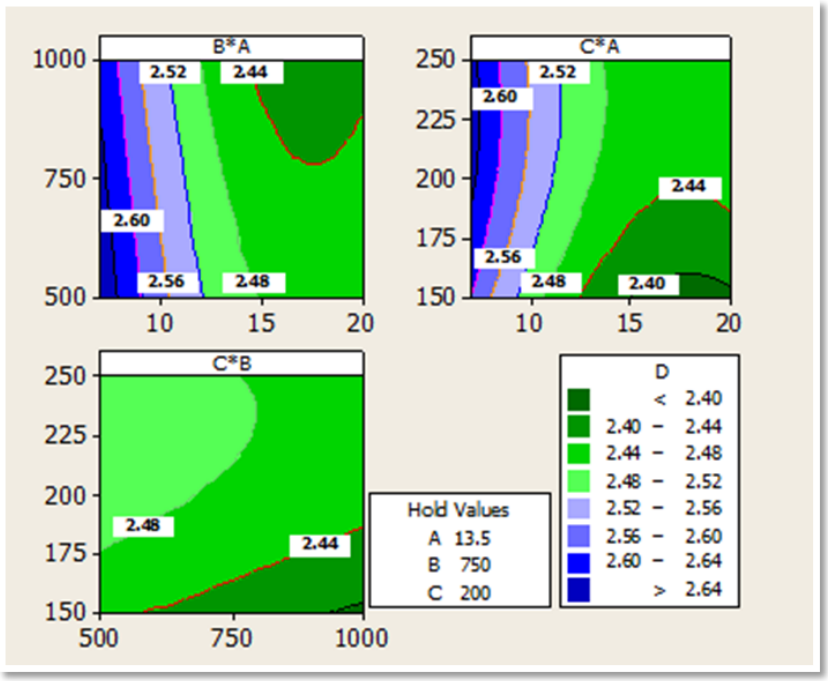

Fig. 12: Two-Dimensional Response Surface Plots for Foam Density.

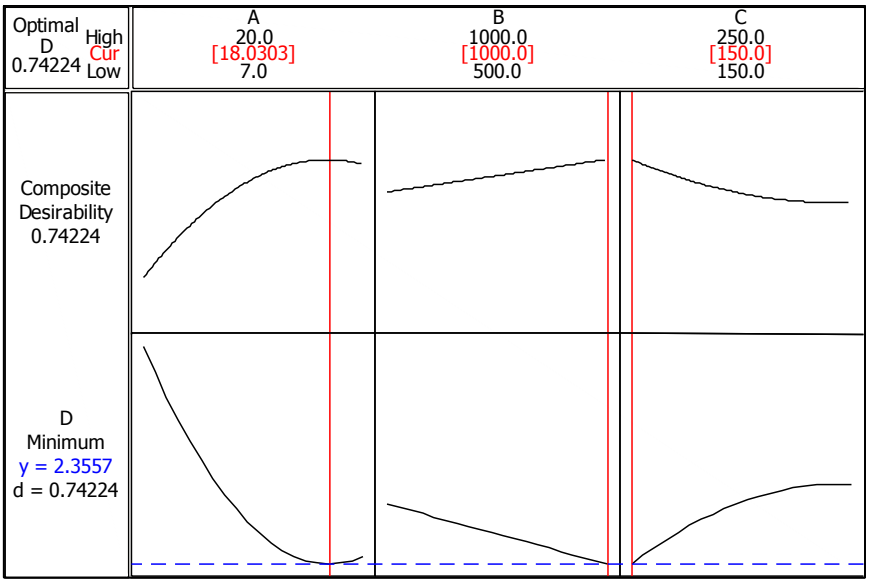

Fig. 13: Response Optimization Plot (Foam Density).

In Figure (14), a two contour-line graph shows the effects on porosity fraction based on % NaCl, NaCl particle size, and compacting pressure. Figure (15) shows the optimum value at the top of the graph at 20%, 1000 μm, and 150 MPa, with a resulting maximum porosity fraction of 26.5946%.

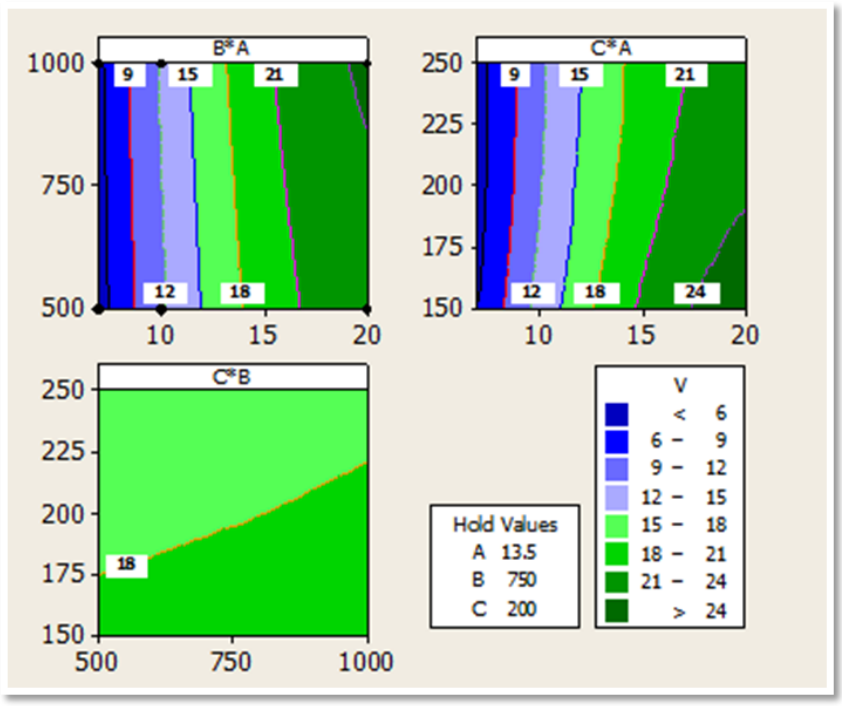

Fig. 14: Two Dimensional Response Surface Plots for Porosity Fraction.

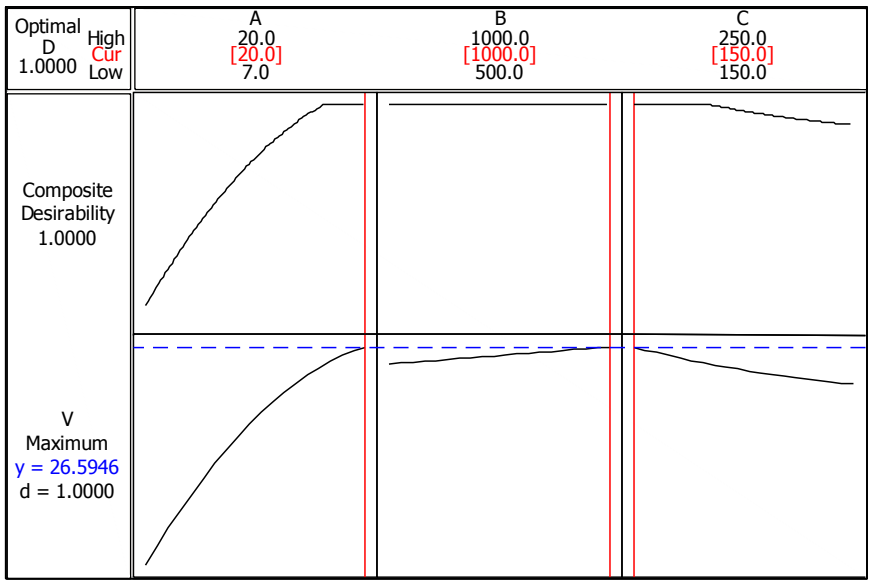

Fig. 15: Response Optimization Plot (Porosity Fraction).

8. Conclusions

This work evaluated the effects of process parameters on Al foams and applied response surface methodology to determine the optimum conditions of % NaCl, NaCl particle size, and compacting pressure for foam density and porosity fraction. The results are shown below:

1) At a compacting pressure of 150MPa and NaCl particle size of 500 µm, the density and porosity fraction are 2.44 g/m^3 and 25.2%, respectively. At a NaCl particle size of 1000 µm, the density and porosity fraction are 2.34 g/m^3 and 26.6%, respectively.
2) Density (ρ_f) decreases and porosity fraction increases as compacting pressure decreases with a constant NaCl particle size and % NaCl.
3) From statistical analysis on foam density, a second-order polynomial equation was confirmed by the ANOVA result, with a P-value lower than 0.05. In numerical optimization, the obtained optimal conditions (i.e., 18.0303%, 1000 µm, and 150 MPa as % NaCl, NaCl particle size, and compacting pressure, respectively) resulted in a minimum foam density of 2.35568 g/cm^3

4) In the same manner, from statistical analysis on porosity fraction, a second-order polynomial equation was confirmed by the ANOVA result, with a P-value lower than 0.05. In numerical optimization, the obtained optimal conditions (i.e., 20%, 1000 μm, and 150 MPa as % NaCl, NaCl particle size, and compacting pressure, respectively) resulted in a maximum porosity fraction of 26.5946%.

Acknowledgements

I express my gratitude to Dr. Nawal Ezzat Abdul-lateef for supporting me in this work.

References

[1] Harikalam Thabarealam, "Production, Processing and Characterisation of Porous TiAl Alloy Produced Using Space Holder Method", *Master thesis, The University of Waikato, Hamilton, New Zealand*, (April 2009), http://waikato.researchgateway.ac.nz/

[2] A.M. Parvanian and M. Panjepour, "Mechanical behavior improvement of open-pore copper foams synthesized through space holder technique", *Materials and Design*, Vol. 49, (2013), pp. 834–841. http://dx.doi.org/10.1016/j.matdes.2013.01.077.

[3] Banhart, John. "Manufacture, characterisation and application of cellular metals and metal foams", *Progress in Materials Science*, Vol. 46, (2001), pp.559–632. http://dx.doi.org/10.1016/S0079-6425(00)00002-5.

[4] A. K. Shaik dawood, S. S. Mohamed Nazirudeen, "A Development of Technology for Making Porous Metal Foams Castings", Vol. 4, No. 2, (2010), pp. 292 – 299.

[5] Masataka Hakamada, Yasuo Yamada, Tatsuho Nomura, Youqing Chen, Hiromu Kusuda and Mamoru Mabuchi, "Fabrication of Porous Aluminum by Spacer Method Consisting of Spark Plasma Sintering and Sodium Chloride Dissolution", *Materials Transactions*, Vol. 46, No. 12, (2005), pp. 2624-2628. http://dx.doi.org/10.2320/matertrans.46.2624.

[6] Michailidis N. and F. Stergioudi, "Establishment of process parameters for producing Al-foam by dissolution and powder sintering method", *Materials and Design*, Vol. 32, (2011), pp. 1559–1564. http://dx.doi.org/10.1016/j.matdes.2010.09.029.

[7] Y.Y. Zhao, D.X. Sun, "A novel sintering-dissolution process for manufacturing Al foams", *Scr. Mater.* Vol. 44, pp. 105-110. http://dx.doi.org/10.1016/S1359-6462(00)00548-0.

[8] Rossella Surace, Luigi A. C. De Filippis, Antonio D. Ludovico and Giancarlo Boghetich, "Experimental analysis of the effect of control factors on aluminium foam produced by powder metallurgy", *Proc. Estonian Acad. Sci. Eng.*, Vol. 13, (2007), pp. 156–167.

[9] Montgomery D.C., Design and analysis of experiments, John Wiley and Sons, NewYork, 1991.